NACA

RESEARCH MEMORANDUM

THE VERTICAL-TAIL LOADS MEASURED DURING A FLIGHT INVESTIGATION ON A JET-POWERED BOMBER AIRPLANE

By T. V. Cooney

Langley Aeronautical Laboratory
Langley Field, Va.

NATIONAL ADVISORY COMMITTEE
FOR AERONAUTICS

WASHINGTON

May 1, 1953

NATIONAL ADVISORY COMMITTEE FOR AERONAUTICS

RESEARCH MEMORANDUM

THE VERTICAL-TAIL LOADS MEASURED DURING A FLIGHT INVESTIGATION ON A JET-POWERED BOMBER AIRPLANE

By T. V. Cooney

SUMMARY

Results are presented of a flight investigation conducted on a jet-powered bomber airplane to determine the vertical-tail loads. Strain-gage measurements were made of the fin and rudder loads in abrupt rudder kicks, and in gradual sideslip maneuvers.

The basic aerodynamic parameters, C_{L_α} and C_{L_δ}, for the vertical tail were determined from time-history measurements of vertical-tail load, sideslip angle, rudder position, and yawing velocity in abrupt rudder kicks by a procedure involving a least-squares solution.

At the first peak load in the rudder kicks the rudder load was about 42 percent of the total vertical-tail load and the fin load was 58 percent of the total load, while at the time of maximum sideslip angle the rudder load was 28 percent of the total load and the fin load in the opposite direction from the rudder load was 128 percent of the total. The total vertical-tail load measured in gradual sideslips was small. However, during these maneuvers the rudder load was $1\frac{1}{2}$ times the total (net) load while the fin load, in the opposite direction, was $2\frac{1}{2}$ times the total vertical-tail load.

Estimates of the vertical-tail-surface loads in an abrupt-rudder-reversal maneuver are made by using the parameters derived from the flight tests.

INTRODUCTION

The theoretical and experimental investigations which have been carried out in recent years have contributed to the understanding of

the problems involved in the design of vertical tail surfaces. Some of the more recent analytical studies have been concerned with the determination of the sideslip angles and rudder deflections which can be attained in various types of maneuvers. (See refs. 1, 2, and 3.) Flight measurements of the vertical-tail loads and a comprehensive study of the factors affecting the loads and the distribution of load on the vertical tail of a fighter-type airplane are presented in reference 4. Reference 5 gives a comparison of the vertical-tail loads measured in flight tests with the loads calculated from the flight measurements of sideslip angles and rudder deflections and the aerodynamic parameters obtained from charts of reference 6. The recent flight investigations, however, including those reported in references 4 and 5, are concerned exclusively with fighter-type aircraft, and the question has arisen as to whether or not the same considerations hold true for larger airplanes.

In order to obtain information on the vertical-tail loads experienced by a bomber-type airplane, a flight investigation was carried out with a B-45A. Strain-gage measurements were made of the loads encountered by the vertical tail surfaces in abrupt rudder-kick maneuvers and in gradual sideslip maneuvers. The loads measured under these conditions of flight are presented in this paper together with the results of an analysis of the data to determine parameters which are involved in the design of vertical tail surfaces.

Particular attention is given to a discussion of the method used for extracting the vertical-tail basic aerodynamic parameters, C_{L_α} and C_{L_δ}, from the flight data obtained in rudder kicks. The portion of the total vertical-tail load carried by the fin and rudder in the various maneuvers was also determined and is presented. An estimate is made of the loads on the vertical tail surfaces in an abrupt rudder reversal maneuver. The estimates are based on measurements made during this flight investigation and are compared with the limit design loads.

SYMBOLS

V	true airspeed, ft/sec
M	Mach number
q	dynamic pressure, lb/ft^2
L_V	vertical-tail aerodynamic load, lb

L_R	rudder aerodynamic load, lb
L_F	fin aerodynamic load, lb
δ_r	rudder deflection, deg
α_V	angle of attack at vertical tail, deg
β	sideslip angle, deg
$\dot{\psi}$	yawing velocity, rad/sec
p	rolling velocity, rad/sec
l	tail length (distance from center of gravity to rudder hinge line), ft
S_V	vertical-tail area, ft^2
C_{L_α}	rate of change of vertical-tail lift coefficient with angle of attack
C_{L_δ}	rate of change of vertical-tail lift coefficient with rudder deflection
L_{V_1}	first peak load in a rudder kick, the deflection load, lb
L_{V_2}	second peak load in a rudder kick, the dynamic load, lb
L_{V_β}	rate of change of vertical-tail load with sideslip, $\frac{\partial L_V}{\partial \beta}$
$L_{V_{\delta_r}}$	rate of change of vertical-tail load with rudder deflection, $\frac{\partial L_V}{\partial \delta_r}$
$L_{V_{\dot{\psi}}}$	rate of change of vertical-tail load with yawing velocity, $\frac{\partial L_V}{\partial \dot{\psi}}$

With any of the above symbols, the prefix Δ represents an increment measured from the trim condition.

APPARATUS AND TESTS

Airplane.- A photograph of the test airplane, a B-45A, is shown in figure 1, and figure 2 shows a three-view drawing with some pertinent dimensions. For this investigation the airplane take-off weight was approximately 65,000 pounds and the weight on landing was approximately 50,000 pounds. The center of gravity varied less than 1 percent mean aerodynamic chord due to fuel consumption during the period of time required for the test runs, and the approximate center-of-gravity position during the test maneuvers was 28 percent mean aerodynamic chord. Figure 3 shows the vertical-tail configuration and the approximate locations of the strain-gage bridges. Also included in figure 3 is a table of the geometric characteristics of the vertical tail surface.

Instrumentation.- For this investigation, standard NACA recording instruments were installed in the airplane to obtain measurements of airspeed, altitude, sideslip angle, control positions, linear accelerations, and angular velocities. Strain gages were employed to measure loads and the output from the strain gages was recorded on an 18-channel oscillograph. A $\frac{1}{10}$-second time pulse was used to correlate the records of all recording instruments. The airspeed head was located on a boom, at the tip of the left wing, and extended approximately one local chord length ahead of the leading edge. The results of a flight calibration of the airspeed system for position error and an analysis of available data for a similar installation indicated a Mach number error of less than ±0.01 throughout the test range. The sideslip-angle transmitter was located on a boom at the right wing tip for the gradual-sideslip flights and on a boom extending forward of the nose of the airplane for the rudder-kick flights. Neither installation was calibrated for inflow effects; however, errors due to these effects are considered to be minimized since the results are presented as incremental sideslip angles. For the abrupt maneuvers, no correction has been applied to the sideslip-angle measurements for the errors due to the location of the transmitter forward of the airplane center of gravity since the errors in measurements due to this effect are estimated to be within the accuracy of the instrument.

The structural loads L_S from the strain-gage measurements were converted to aerodynamic loads L_A by the addition of an inertia load L_I as indicated by the equation: $L_A = L_S + L_I$. The inertia load is equal to the weight of the tail outboard of the strain-gage station multiplied by the transverse acceleration measured at the root of the vertical tail.

Flight tests.- The flight investigation consisted of rudder-kick maneuvers performed in the Mach number range from 0.40 to 0.74 at 30,000 feet and gradual sideslips in the Mach number range from 0.30 to 0.76 at two altitudes, 20,000 feet and 30,000 feet.

In the rudder-kick maneuvers, the rudder was displaced abruptly and then held in the displaced position while the sideslip angle increased to a maximum value corresponding to the rudder deflection. No appreciable change in airspeed or altitude occurred during these maneuvers.

The sideslip maneuvers were performed by gradually increasing the sideslip in nonturning flight while the airspeed was maintained constant. In all the sideslip maneuvers the sideslip angles were increased until limited either by rudder-pedal travel or by pilot effort. In these maneuvers nearly steady sideslipping conditions prevailed at each instant since the change in sideslip angle was less than $\frac{1^\circ}{2}$ per second. At the start of both the rudder kicks and the gradual sideslips, the airplane was in the clean condition and trimmed for steady flight.

RESULTS AND DISCUSSION

Rudder Kicks in Level Flight

Time histories of the various quantities measured in a typical rudder kick are shown in figure 4. As seen in this figure the rudder was kicked abruptly and then held until after the sideslip angle reached a maximum value. The first peak vertical-tail load (L_{V_1} in fig. 4) will be called the "deflection load" as in reference 6 and the second peak load (L_{V_2} in fig. 4) will be called the "dynamic load."

For a rudder kick in level flight the increment in vertical-tail load over the value of steady load prior to the maneuver can be expressed by the following equation:

$$\Delta L_V = L_{V_\beta} \Delta\beta + L_{V_{\delta_r}} \Delta\delta_r + L_{V_{\dot{\psi}}} \Delta\dot{\psi} \qquad (1)$$

where

$$\left.\begin{aligned} L_{V_\beta} &= C_{L_\alpha} \frac{\alpha_V}{\beta} qS_V \\ L_{V_{\delta_r}} &= C_{L_\delta} qS_V \\ L_{V_{\dot{\psi}}} &= C_{L_\alpha} qS_V \frac{l}{V} \end{aligned}\right\} \qquad (2)$$

If there was appreciable rolling motion present, another term $L_{V_p} \Delta p$ would have to be added to account for the angle-of-attack increment contributed by the rolling velocity. Since only incremental vertical-tail loads are considered throughout this paper, effects of fin offset or any other unsymmetry built into the airplane which would affect the absolute value of the vertical-tail loads do not appear in the equation.

From the measurements of vertical-tail load, sideslip angle, rudder position, and yawing velocity such as those shown in the time history of figure 4, readings were made of each quantity at $\frac{1}{10}$-second intervals. Each reading was then subtracted from the value of the corresponding measurement which existed at the start of the maneuver (time, 0.3 sec, in fig. 4). The incremental values thus obtained were substituted into equations of the form of equation (1) which were then solved by a least-squares procedure for the coefficients L_{V_β}, $L_{V_{\delta_r}}$, and $L_{V_{\dot{\psi}}}$. The $\frac{1}{10}$-second increment for reading the records was chosen for convenience; however, any increment other than $\frac{1}{10}$ second could have been selected. It is necessary to have the number of readings large in comparison with the number of unknown coefficients to be evaluated because the accuracy of the determined coefficients increases as the number of readings increases.

The method used to solve for the coefficients of equation (1) assumes that there is linear dependence of the incremental vertical-tail

load on the sideslip angle, rudder deflection, and yawing velocity and that these three variables adequately define the vertical-tail angle of attack at any instant. The validity of these assumptions is indicated in figure 5 where the measured incremental load from figure 4 is compared with the vertical-tail load computed by using equation (1) and the coefficients determined by the method outlined.

From figure 5 it can be seen that the magnitude of the vertical-tail load is duplicated throughout the maneuver; hence, it may be concluded that β, δ_r, and $\dot{\psi}$ are the only important influencing variables. Values of L_{V_β}, $L_{V_{\delta_r}}$, and $L_{V_{\dot{\psi}}}$ were obtained from the solution of equations of the type of equation (1) for each of the 26 rudder-kick runs made at the various values of dynamic pressure and rates of rudder deflection.

From equations (2), C_{L_α} and C_{L_δ} may be calculated as

$$C_{L_\alpha} = \frac{L_{V_\beta}}{qS_V} \tag{3}$$

and

$$C_{L_\delta} = \frac{L_{V_{\delta_r}}}{qS_V} \tag{4}$$

if the assumption is made that the sidewash factor α_V/β is equal to unity. The vertical-tail area used here is the shaded area in figure 3 which is the portion of the vertical tail outboard of the strain-gage location.

The variation of C_{L_α} and C_{L_δ} with Mach number as determined from equations (3) and (4) is shown in figure 6. The increase in lift-curve slope C_{L_α} with Mach number which is evident in figure 6 is of the magnitude to be expected from the commonly used compressibility correction factor $\frac{1}{\sqrt{1 - M^2}}$. However, the values of C_{L_α} shown in figure 6 as well as the magnitude of the variation with Mach number are dependent on the assumption that α_V/β is equal to unity. An additional

consideration is the fact that all the flight measurements were made at one altitude and the changes in Mach number in figure 6 also correspond to changes in airplane lift coefficient as well. Experimental information given in reference 7 indicates that the effective vertical-tail lift-curve slope decreases with increasing angle of attack.

The vertical tail has a geometric aspect ratio of 1.35 but due to the end-plate effect of the horizontal tail it has an effective aspect ratio of 2.08 determined by multiplying the geometric value by 1.55 according to reference 6. Corresponding to this effective aspect ratio, figure 3 of reference 6 would indicate a lift-curve slope of 0.045 whereas the value of C_{L_α} shown in figure 6 for the lowest test Mach number is 0.029.

Since there is no appreciable variation in C_{L_δ} with Mach number shown in figure 6, and since C_{L_α} increases with increasing Mach number, rudder effectiveness $C_{L_\delta}/C_{L_\alpha}$ is reduced with increasing Mach number.

Deflection load.- In an abrupt rudder kick the first peak vertical-tail load usually occurs before the airplane has had a chance to sideslip. When this is the case β and $\dot{\psi}$ are zero and equation (1) reduces to

$$\Delta L_V = \Delta L_{V_1} = L_{V_{\delta_r}} \Delta\delta_r = C_{L_\delta} \Delta\delta_r \, qS_V \tag{5}$$

The increment in vertical-tail deflection load ΔL_{V_1} was divided by the rudder deflection responsible for it and this ratio is plotted against the dynamic pressure of the maneuver in figure 7. In this figure each point represents the value of $\frac{\Delta L_{V_1}}{\Delta\delta_r}$ determined for one rudder-kick run including various rates of rudder deflection from 20° per second to 50° per second. In each case, however, the rudder rate was sufficiently great to allow the load to reach a peak value while the airplane was still undisturbed in sideslip. The variation of $\frac{\Delta L_{V_1}}{\Delta\delta_r}$ with q is a measure of the lift coefficient due to rudder deflection C_{L_δ} multiplied by the vertical-tail area. The solid line in figure 7 shows how the value of $C_{L_\delta}S_V$ previously obtained from the least-squares analysis considering the entire rudder-kick run compares with the peak "deflection" load divided by the rudder deflection.

Although chordwise distributions of load were not measured, the rudder hinges were instrumented so that the load carried by the rudder and transmitted through the hinges was measured. The measured incremental rudder load for the first load peak in rudder kicks is plotted against the incremental total vertical-tail load in figure 8. It can be seen from this figure that for the so-called deflection load, 42 percent of the total load is carried by the rudder and 58 percent is carried by the fin. The rudder carries a constant percent of the total load for various dynamic pressures and for Mach numbers up to $M = 0.74$.

Dynamic load.- The second peak load of figure 4, called the dynamic load, coincides with the time of occurrence of the greatest sideslip angle in rudder-kick maneuvers where the rudder was deflected abruptly to some position and then held until after the peak sideslip angle was attained. At the time of greatest sideslip angle $\Delta\dot{\psi}$ is approximately equal to zero, and equation (1) reduces to

$$\Delta L_V = \Delta L_{V_2} = L_{V_\beta} \Delta\beta + L_{V_{\delta_r}} \Delta\delta_r \tag{6}$$

From equation (6) it can be seen that the dynamic load is made up of a component of the load due to sideslip and a component due to the deflected rudder. These two loads act in opposite directions. If the rudder were to be returned to zero at any time during the maneuver after the sideslip had begun to build up, the resultant load would be greater since the relieving load due to the deflected rudder would be absent. A still greater load would be obtained if the maneuver were checked by reversing the rudder at the time of maximum sideslip.

Equation (6) can also be written as

$$\frac{\Delta L_{V_2}}{\Delta\delta_r} = L_{V_\beta} \frac{\Delta\beta_{max}}{\Delta\delta_r} + L_{V_{\delta_r}} \tag{7}$$

which expresses the dynamic load per degree rudder deflection in terms of the coefficients L_{V_β} and $L_{V_{\delta_r}}$ and the term $\frac{\Delta\beta_{max}}{\Delta\delta_r}$, the maximum sideslip angle resulting from a given rudder deflection. The magnitude of $\frac{\Delta\beta_{max}}{\Delta\delta_r}$ for an abrupt maneuver depends on the airplane damping in yaw and is generally from 1.5 to 2.0 times the value resulting in steady sideslip maneuvers where the yawing velocity is zero. For the test airplane,

the ratio of $\frac{\Delta\beta_{max}}{\Delta\delta_r}$ in the rudder kicks to the value of $\frac{\Delta\beta}{\Delta\delta_r}$ in sideslips was found from the flight tests to be approximately 1.5.

The variation of the dynamic load per degree rudder deflection with q for each rudder-kick run is shown in figure 9. The variation of the incremental rudder load with the incremental total vertical-tail load is shown in figure 10. It can be deduced from figure 10 that for the dynamic load the rudder carries approximately 28 percent of the total load and since the fin load acts in the opposite direction it carries 128 percent of the total load.

Gradual Sideslips

The gradual-sideslip maneuvers performed in this investigation were not strictly steady-state maneuvers; however, the rate of increase of sideslip was so low that the yawing velocity was negligible and the airplane could be considered to be in a balanced flight condition. In each of the sideslip maneuvers performed the pilot gradually increased the sideslip until he was prevented from further increases by limiting rudder-pedal travel or maximum rudder-pedal travel limited by pilot effort. At the test altitudes, the loads and control deflections obtained in the sideslip maneuvers were therefore the greatest obtainable by the pilot in this type of maneuver. Full rudder-pedal travel did not result in full deflection of the rudder due to cable stretch. A time history of the various quantities measured in a representative sideslip maneuver is shown in figure 11.

To maintain equilibrium at each instant in a steady sideslip condition, there is a definite relationship between sideslip angle and rudder position which is a characteristic of a given airplane. The particular rudder position is that needed to provide the vertical-tail load necessary to balance the airplane yawing moment in sideslip.

Because of this interdependence of the rudder position, sideslip angle, and vertical-tail load, the aerodynamic coefficients Lv_β and so forth cannot be deduced from the gradual-sideslip data as was done in the case of the rudder kicks. To further explain this point, consider equation (1) when the yawing velocity is zero: $\Delta L_V = Lv_\beta \Delta\beta + Lv_{\delta_r} \Delta\delta_r$. For any given position of the rudder there is a resulting sideslip angle and vertical-tail load. For any other position of the rudder the airplane would assume another sideslip angle which would result in a new value of vertical-tail load. Each term of the equation which represents this second condition will be a multiple of the corresponding term in the equation which represents the first condition, except for small errors due to

inaccuracies in the various measurements. The resulting equations which would be written if a least-squares solution were attempted would then be redundant.

For the B-45 airplane the maximum values of the incremental fin, rudder, and total vertical-tail loads obtained in the gradual-sideslip maneuvers at various Mach numbers and at two altitudes are shown in figure 12. It can be seen from figure 12 that the fin and rudder loads are in opposite directions and that the rudder carries approximately $1\frac{1}{2}$ times the total load, and the fin carries $2\frac{1}{2}$ times the total load.

The incremental rudder deflection and sideslip angles associated with these maximum values of load are presented in figure 13. It can be seen from figure 13 that at 20,000 feet the rudder angle available was reduced from 20° at $M = 0.32$ to 6° at $M = 0.76$ due to cable stretch and limiting pilot effort. At the same time the sideslip angles resulting from these rudder deflections were 12.5° at $M = 0.32$ and 3.5° at $M = 0.76$. Slightly greater rudder deflections and sideslip angles were obtained at 30,000 feet at a given Mach number since the loads and rudder forces were smaller under these conditions.

The variation of sideslip angle with rudder deflection for $M = 0.60$ at two altitudes, 20,000 feet and 30,000 feet, is shown in figure 14. From this type of plot, the rate of change of sideslip angle per degree rudder deflection $\frac{\Delta\beta}{\Delta\delta_r}$ was determined and is shown plotted against Mach number in figure 15.

Figure 16 shows the variation of measured increment in fin and rudder load per unit q with increment in sideslip angle at $M = 0.60$ for altitudes of 20,000 feet and 30,000 feet. The variation with Mach number of the incremental vertical-tail load and the incremental fin and rudder loads per unit dynamic pressure and unit sideslip angle for the two altitudes is shown in figure 17. Each point in figure 17 represents the slope of the curve of measured load per q plotted against sideslip angle as shown in figure 16.

Estimated Vertical-Tail Loads in an Abrupt-Rudder-Reversal Maneuver

During the flight investigation rudder kicks and gradual sideslips were selected as the test maneuvers since they would provide the desired loads and control-position measurements without resulting in critical loads on the vertical tail surfaces. From these maneuvers sufficient

information was obtained for estimates to be made of the loads to be expected on the vertical tail surfaces in more critical maneuvers.

A horizontal-plane maneuver which would result in both maximum fin loads and maximum rudder loads is one in which the rudder is abruptly deflected to its limiting position and then held until maximum sideslip is developed at which time the rudder is returned through neutral to full opposite deflection. Figure 18 illustrates the loads which might be expected to result from this hypothetical maneuver. The fin and rudder loads as well as representative type load distributions at four stages of the maneuver are shown in figure 18. The loads shown in the figure apply at altitudes of 30,000 feet and were calculated by using the maximum rudder positions, sideslip angles, and vertical-tail lift coefficients previously determined from analysis of the flight measurements. For comparison, the limit design loads calculated by the manufacturer using the applicable loading requirements are included in figure 18. It can be seen from the figure that the loads obtained by application of these requirements would not be exceeded in this hypothetical rudder-reversal maneuver at 30,000 feet. Since the amount of rudder deflection available to the pilot and, therefore, the maximum sideslip angles which result are proportional to the dynamic pressure, it is to be expected that the limit loads would not be exceeded in this type of maneuver at altitudes other than 30,000 feet.

CONCLUDING REMARKS

The basic aerodynamic parameters, C_{L_α} and C_{L_δ}, for the vertical tail were determined from time-history measurements of vertical-tail load, sideslip angle, rudder position, and yawing velocity in rudder kicks by a procedure involving a least-squares solution. The magnitude of C_{L_α} obtained from this analysis is dependent on the assumed value of the sidewash factor, α_V/β.

In rudder kicks, the rudder load was 42 percent of the total vertical-tail load and the fin load was 58 percent of the total load at the first peak load, while at the second peak load the rudder load was 28 percent of the total load and the fin load was 128 percent of the total, in the opposite direction.

The total vertical-tail loads measured in gradual sideslips were small. However, during these maneuvers the rudder load was $1\frac{1}{2}$ times

the total (net) load while the fin load was $2\frac{1}{2}$ times the total (net) load, in the opposite direction from the rudder load.

Estimates of the vertical-tail-surface loads in an abrupt-rudder-reversal maneuver were made by using the parameters derived from the flight tests. At an altitude of 30,000 feet the fin and rudder loads were found to be less than the limit design loads for the test airplane during this type of maneuver.

Langley Aeronautical Laboratory,
National Advisory Committee for Aeronautics,
Langley Field, Va.

REFERENCES

1. Czaykowski, T.: Dynamic Fin and Rudder Loads in Yawing Manoeuvres. Rep. No. Structures 76, British R.A.E., June 1950.

2. White, Maurice D., Lomax, Harvard, and Turner, Howard L.: Sideslip Angles and Vertical-Tail Loads in Rolling Pull-Out Maneuvers. NACA TN 1122, 1947.

3. Clousing, Lawrence A.: Research Studies Directed Toward the Development of Rational Vertical-Tail-Load Criteria. Jour. Aero. Sci., vol. 14, no. 3, March 1947, pp. 175-182.

4. Boshar, John: Flight Investigation on a Fighter-Type Airplane of Factors Which Affect the Loads and Load Distributions on the Vertical Tail Surfaces During Rudder Kicks and Fishtails. NACA Rep. 885, 1947. (Formerly NACA TN 1394.)

5. Turner, Howard L.: A Comparison With Flight Data of Vertical-Tail Loads in Various Maneuvers Estimated From Sideslip Angles and Rudder Deflections. NACA RM A7F25, 1947.

6. Pass, H. R.: Analysis of Wind-Tunnel Data on Directional Stability and Control. NACA TN 775, 1940.

7. Dingeldein, Richard C.: Full-Scale Tunnel Investigation of the Pressure Distribution Over the Tail of the P-47B Airplane. NACA ARR 3E25, 1943.

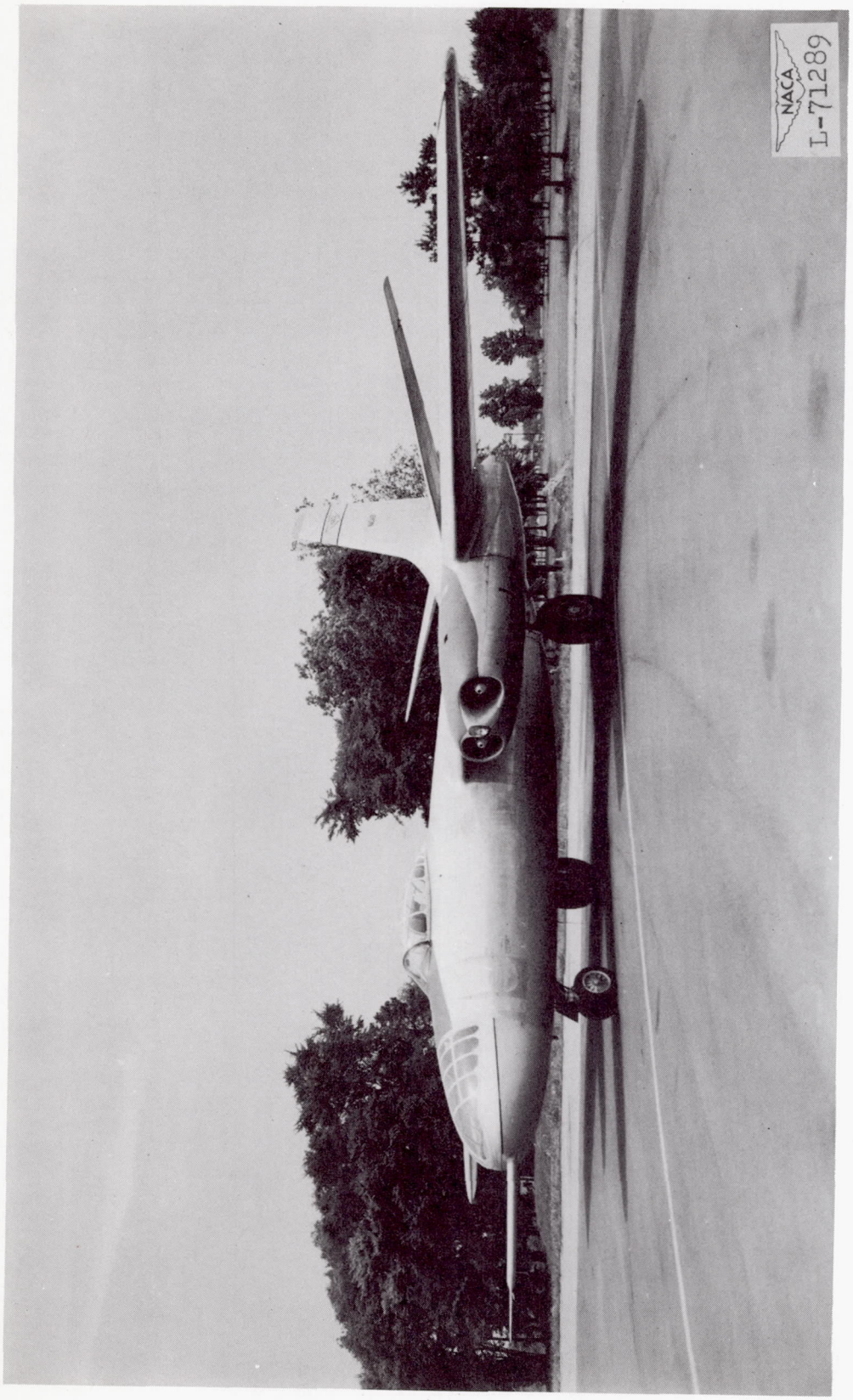

Figure 1.- Photograph of test airplane.

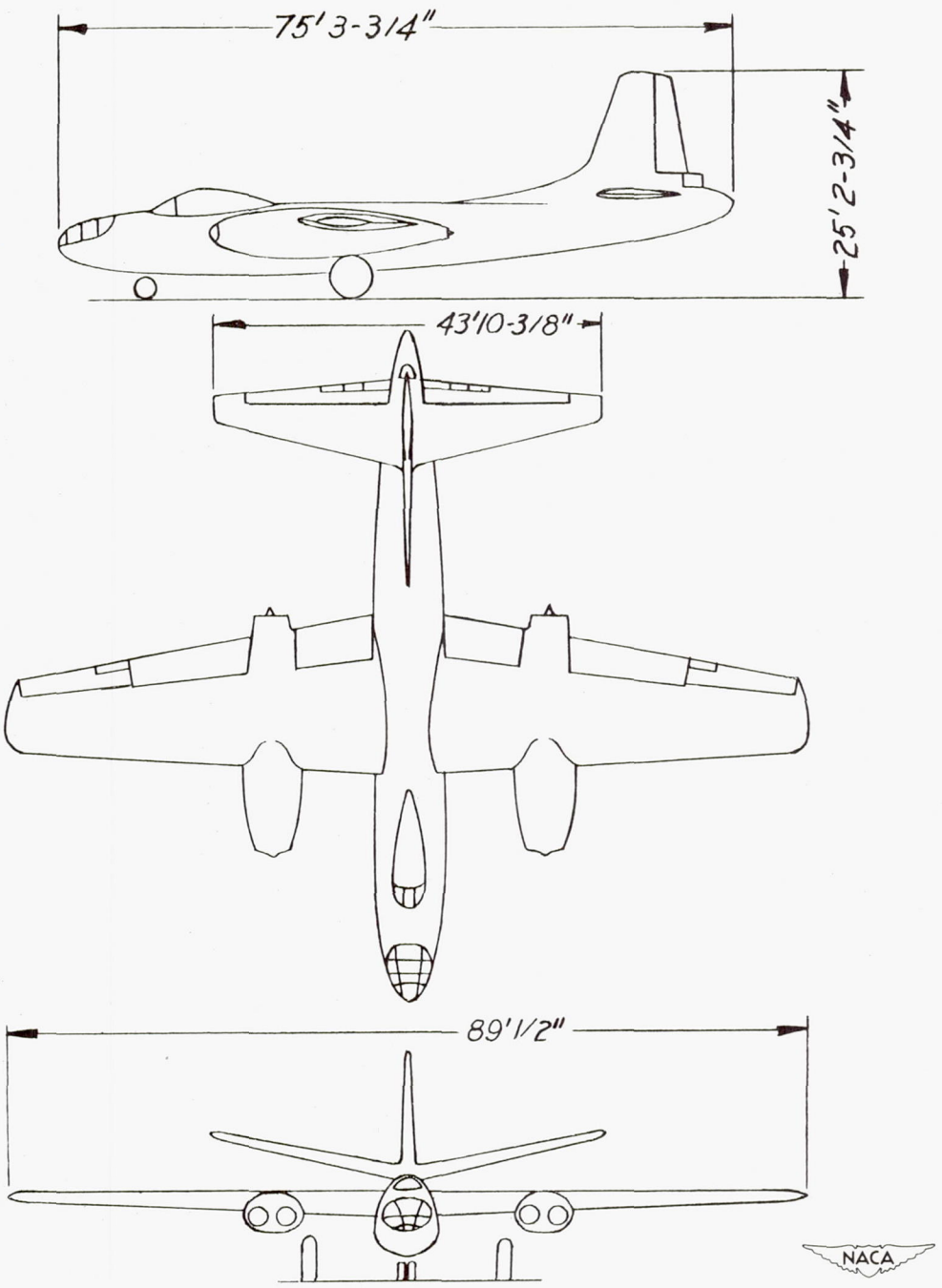

Figure 2.- Three-view drawing of test airplane.

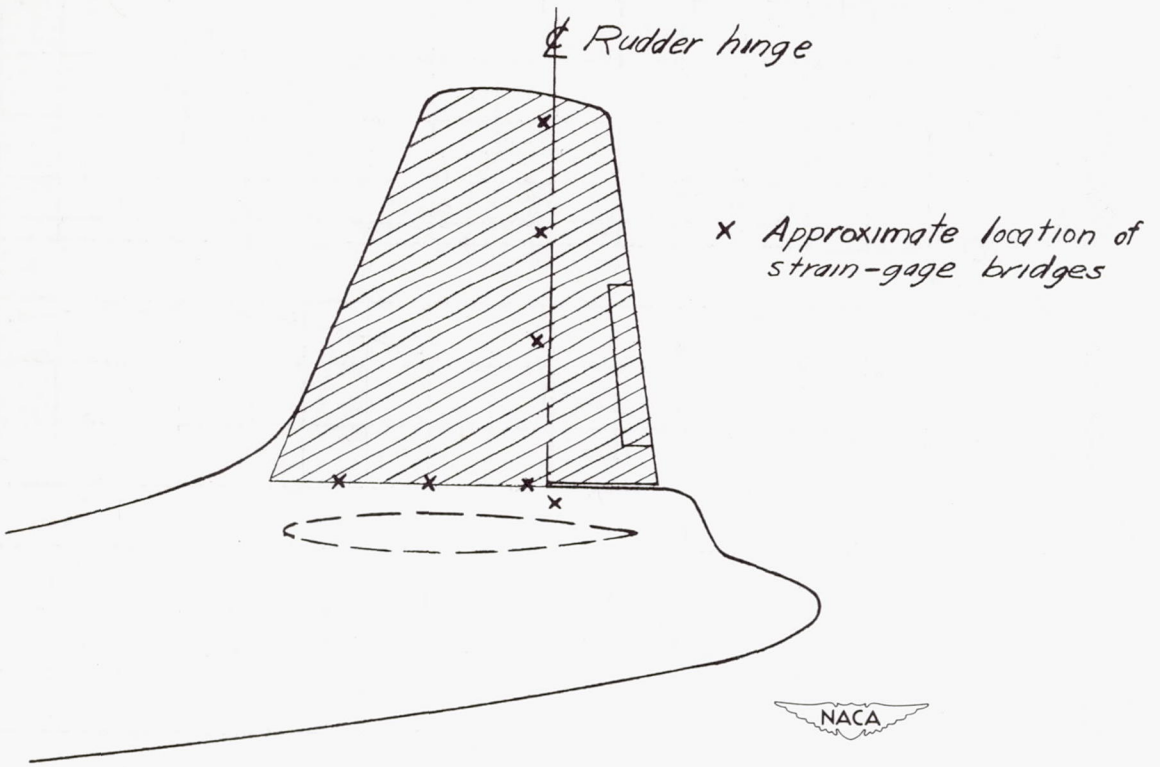

VERTICAL-TAIL GEOMETRY

Airfoil section at root	NACA 65_1-012
Airfoil section at tip	NACA 65-010
Rudder and tab area, sq ft	28
Total area of vertical tail extending above strain-gage location, sq ft	96
Span extending above horizontal tail, in.	150
Location of strain-gage bridges above horizontal tail, in.	13.6
Chord at attachment to horizontal tail, in.	145
Chord at tip, in.	64
Fin offset, deg	0

Figure 3.- Vertical tail surface of test airplane.

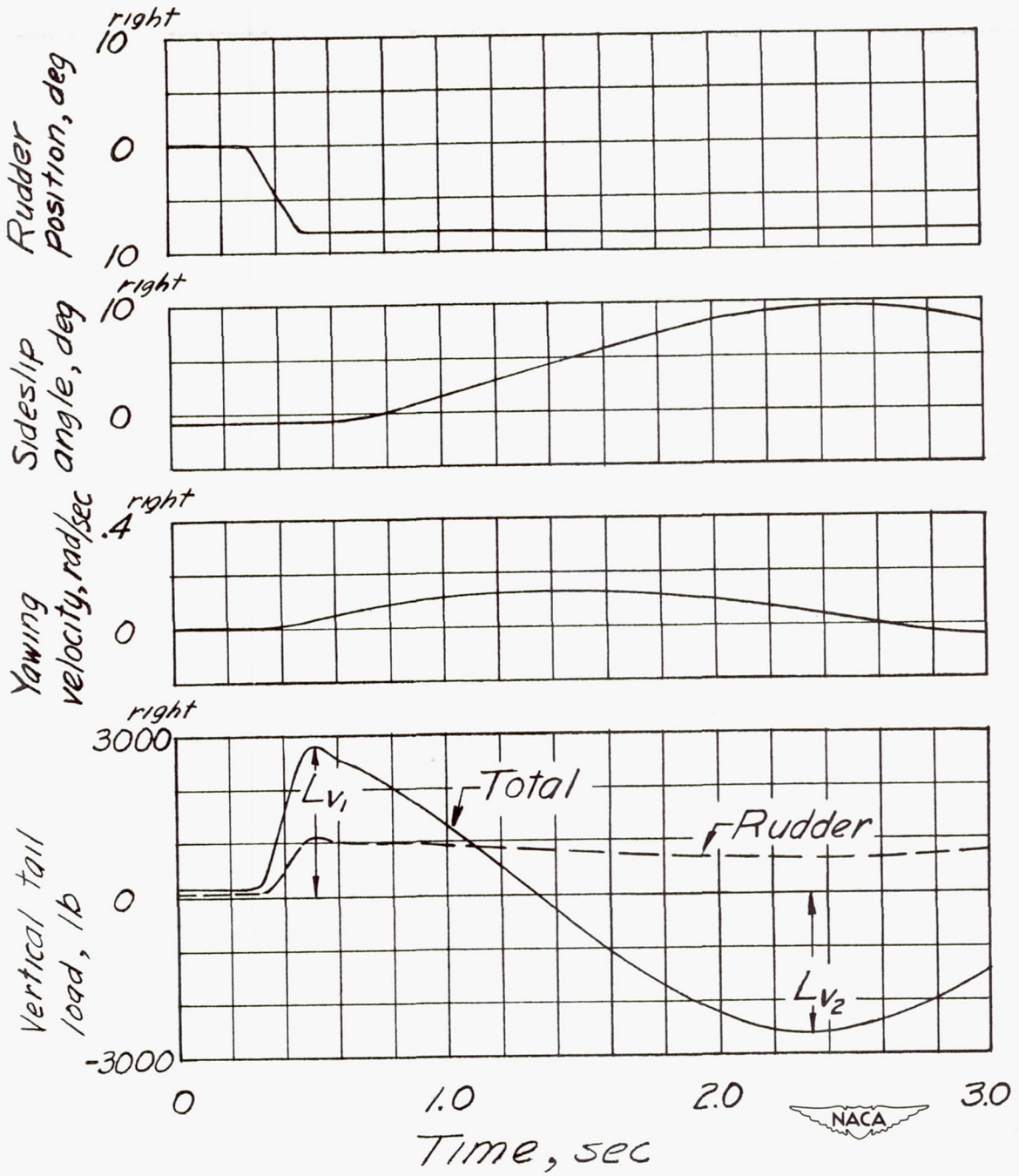

Figure 4.- Time history of the various quantities measured during an abrupt rudder kick. Approximate altitude, 30,000 feet; Mach number, 0.61.

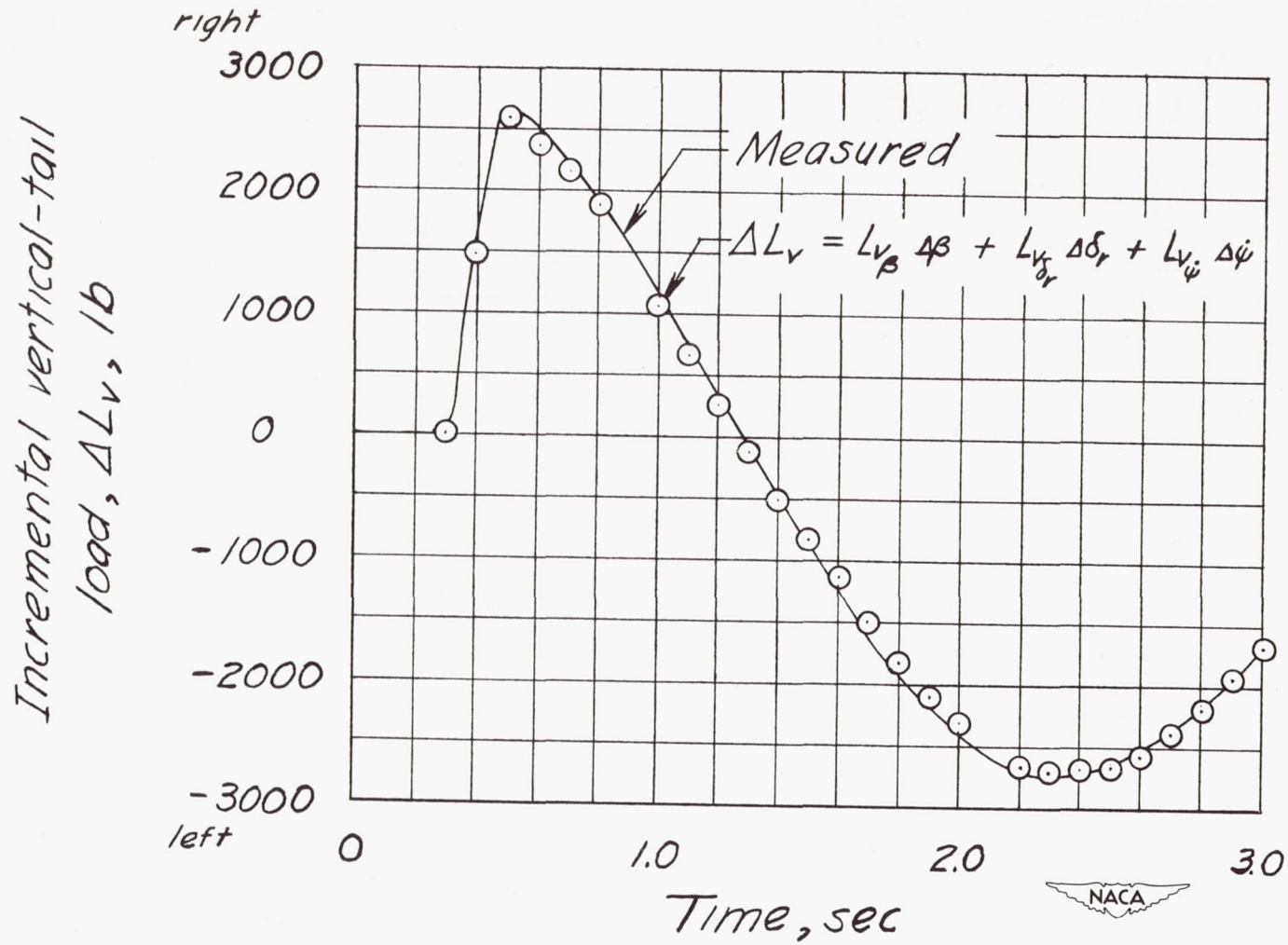

Figure 5.- Comparison of measured vertical-tail load with sum of components due to rudder deflection, sideslip angle, and yawing velocity. Approximate altitude, 30,000 feet; Mach number, 0.61.

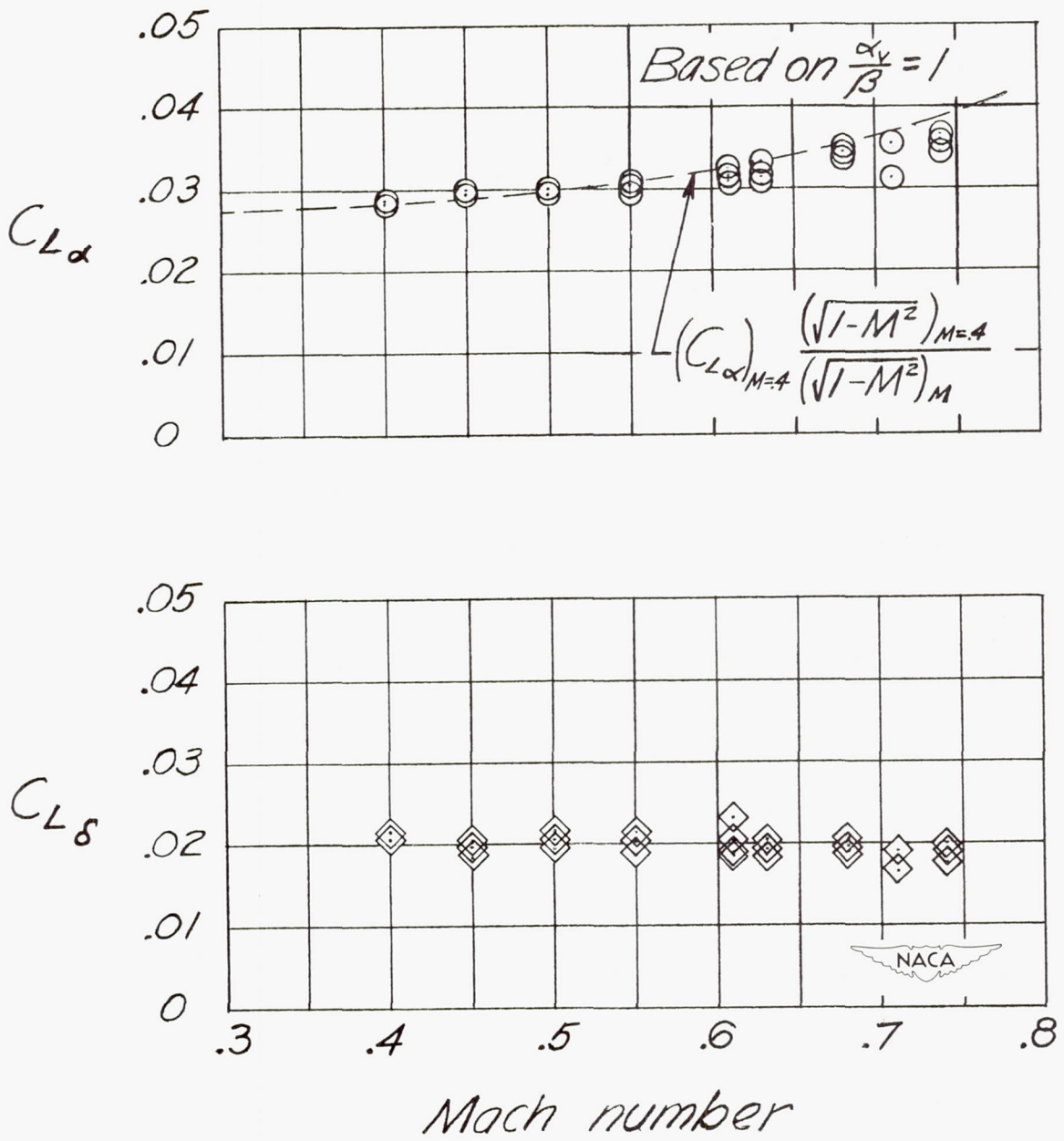

Figure 6.- Variation with Mach number of the lift-coefficient parameters C_{L_α} and C_{L_δ} determined from analysis of vertical-tail loads measured in rudder kicks at 30,000 feet.

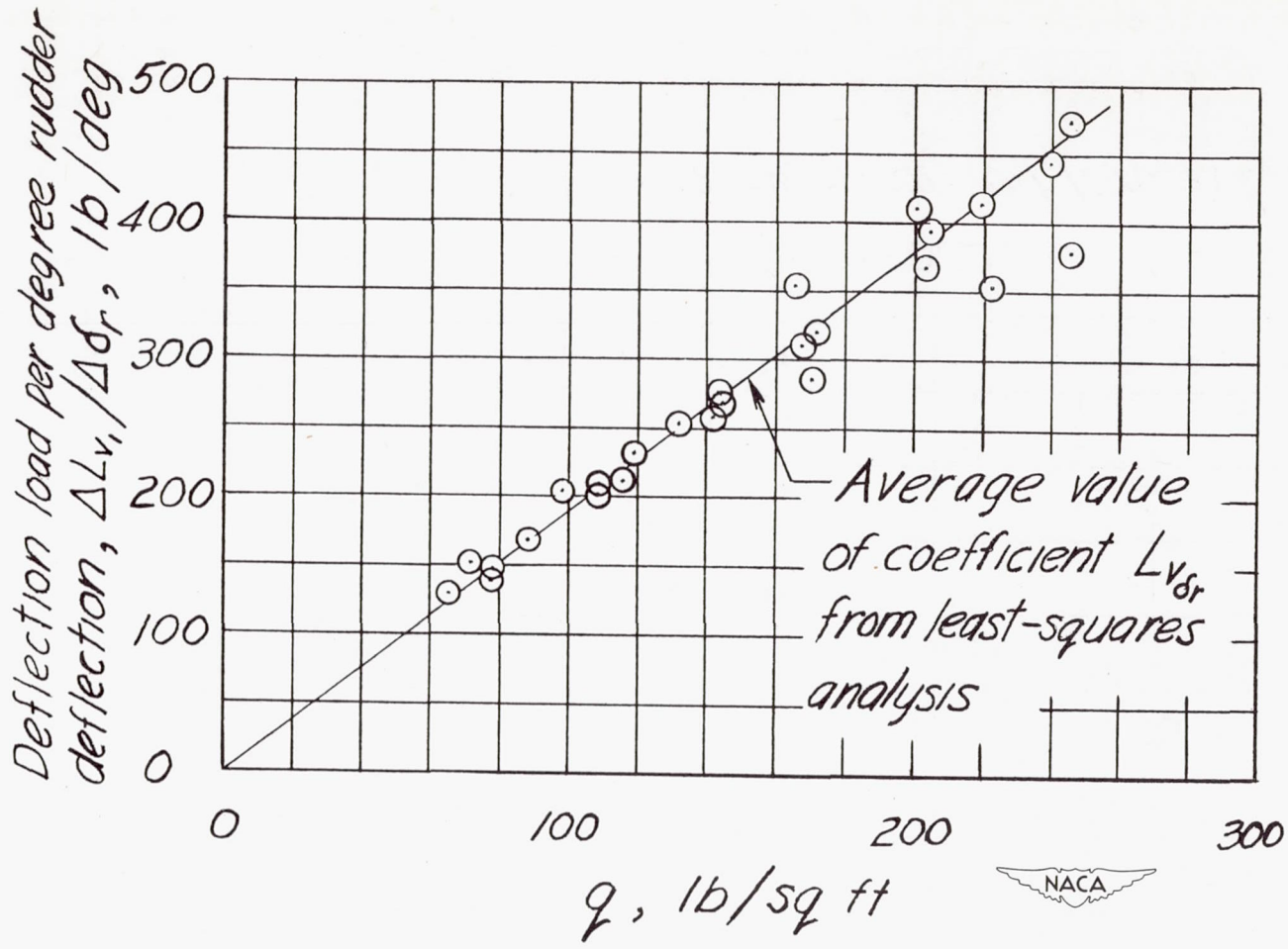

Figure 7.- Variation with dynamic pressure of the deflection load per degree rudder deflection compared with average value of coefficient $L_{v_{\delta_r}}$ obtained from least-squares analysis.

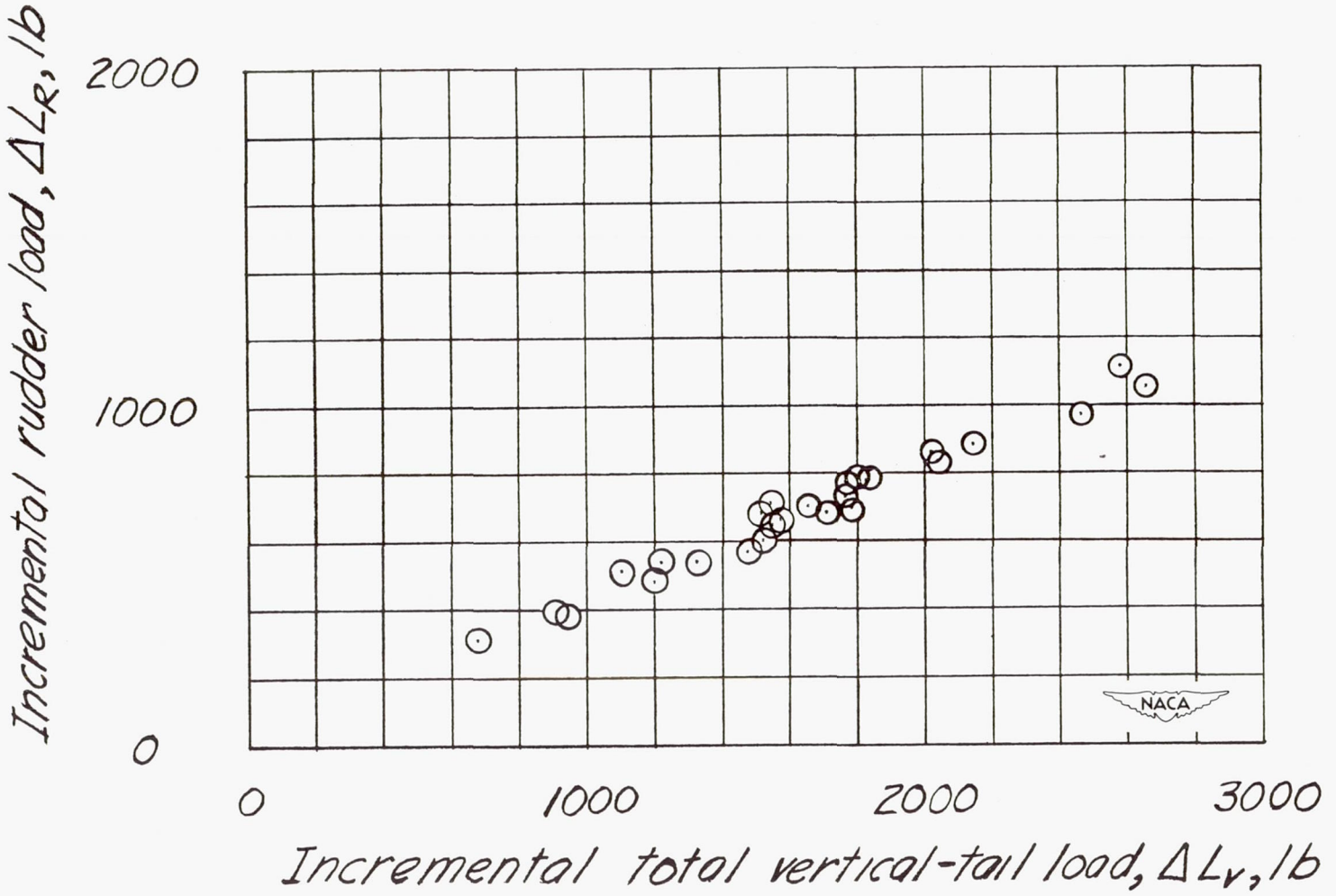

Figure 8.- Variation of incremental rudder load with incremental total vertical-tail load for first peak load in rudder kicks.

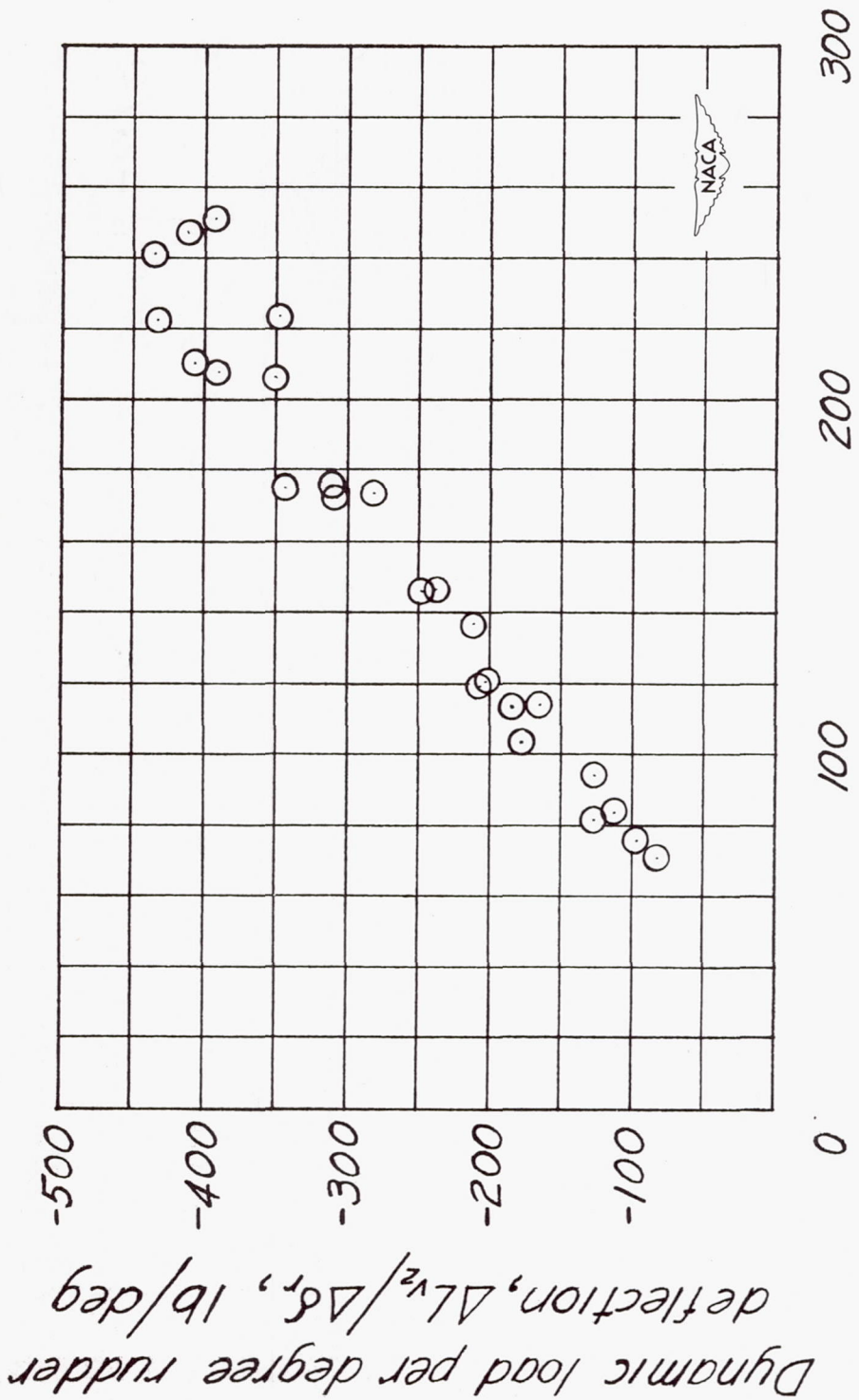

Figure 9.- Variation with dynamic pressure of the dynamic load per degree rudder deflection.

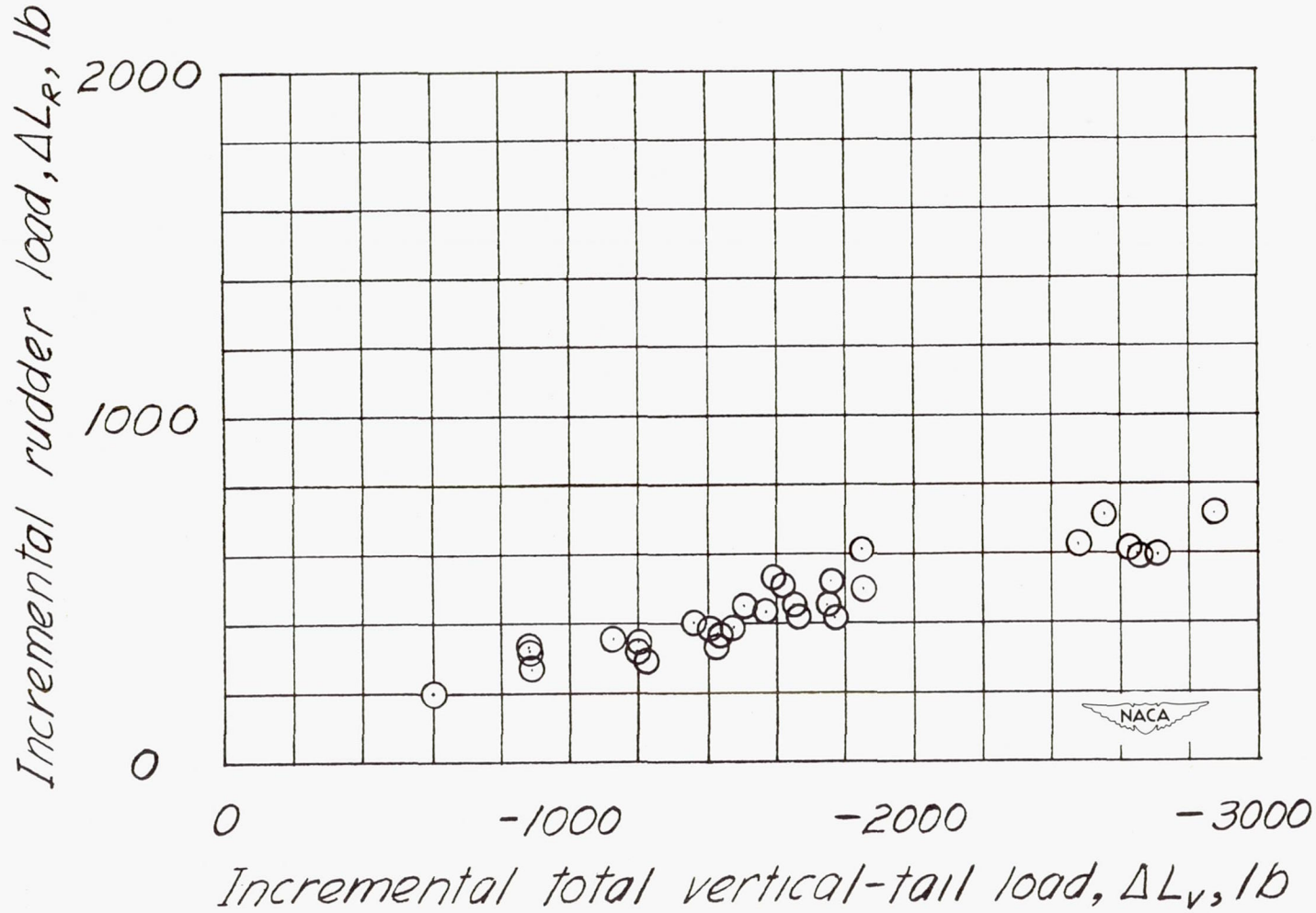

Figure 10.- Variation of incremental rudder load with incremental total vertical-tail load for second peak load in rudder kicks.

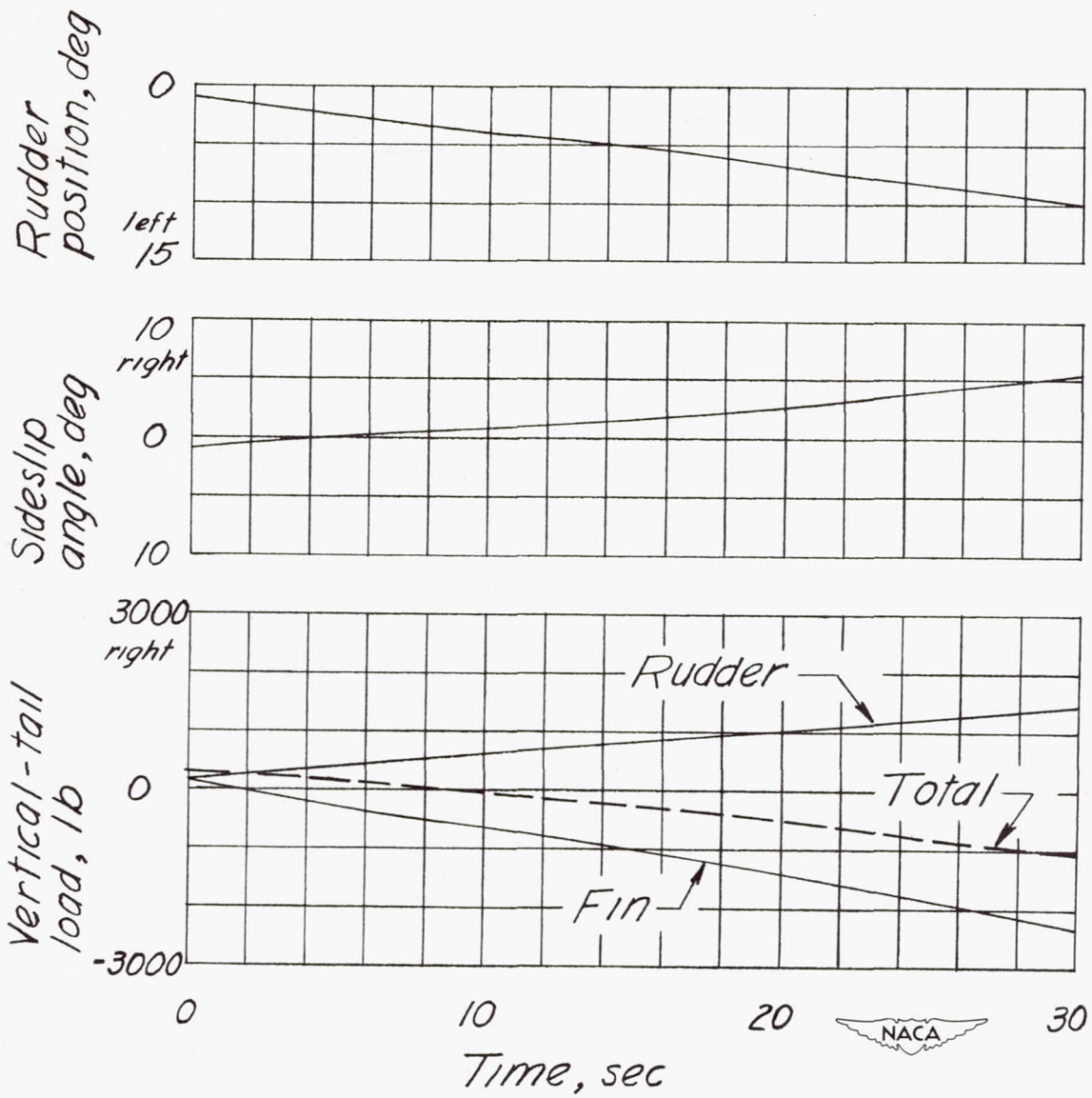

Figure 11.- Time history of the various quantities measured during a gradual sideslip. Approximate altitude, 20,000 feet; Mach number, 0.62.

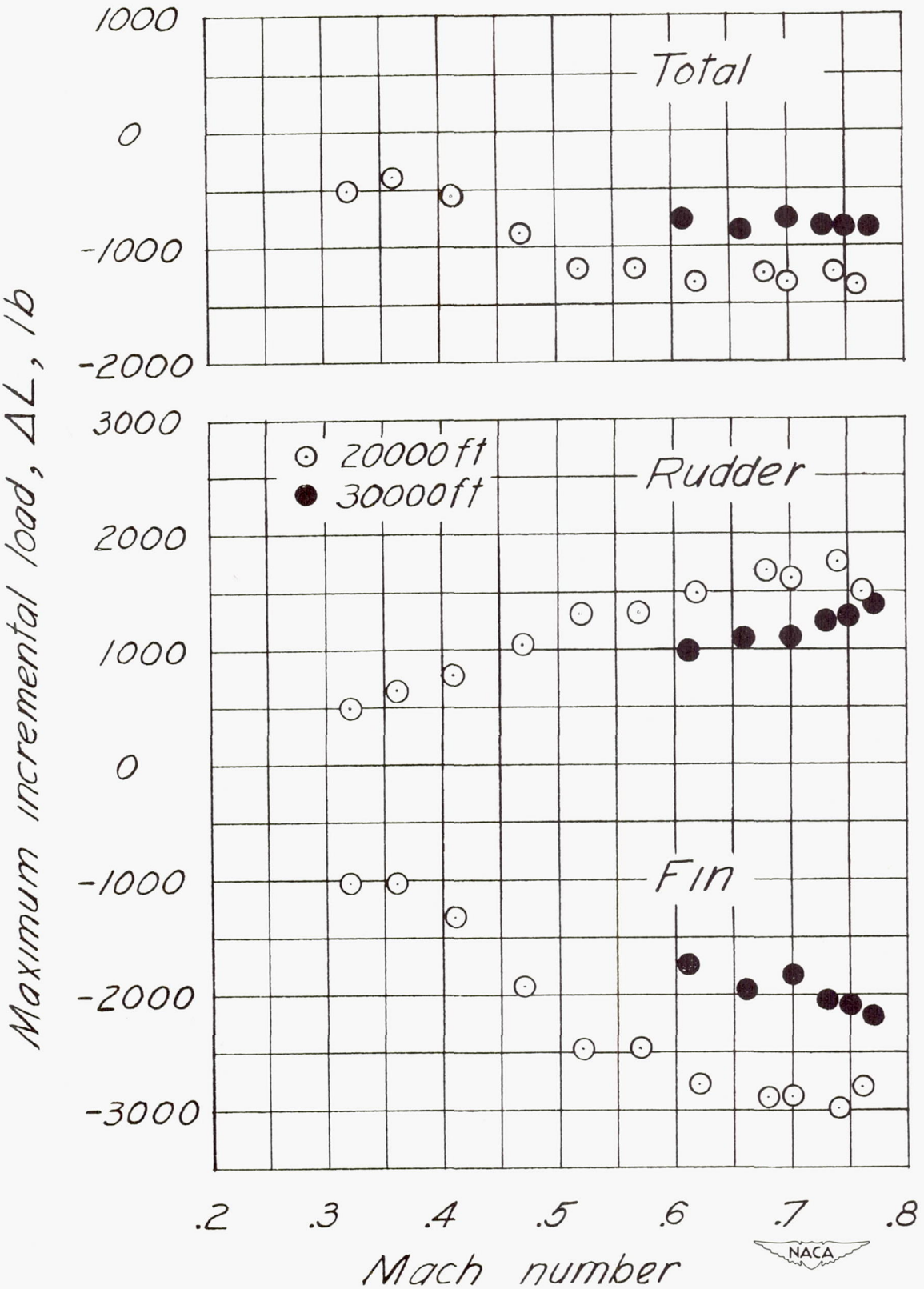

Figure 12.- Variation with Mach number of the maximum incremental total, fin, and rudder loads measured in gradual sideslips at two altitudes.

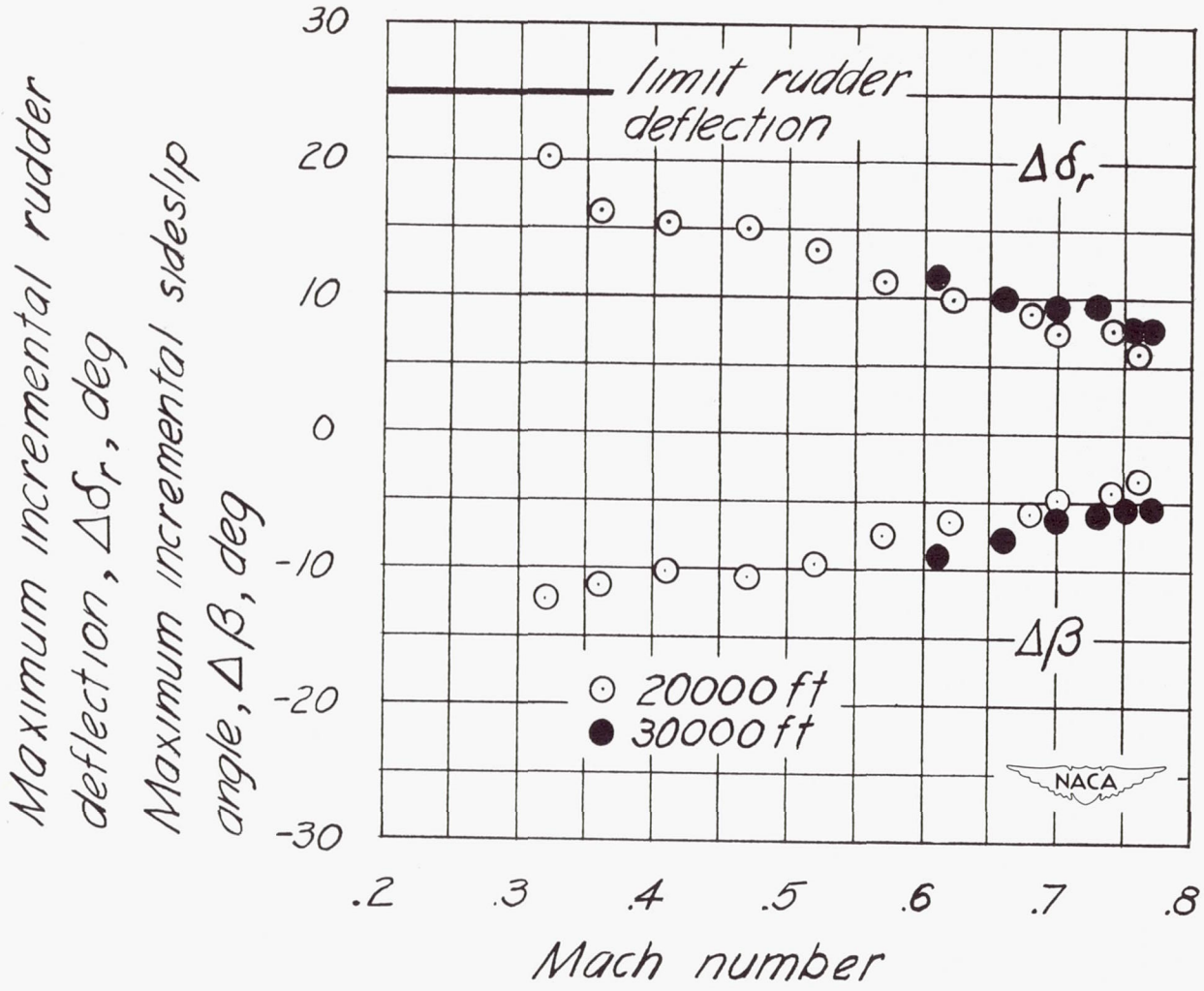

Figure 13.- Variation with Mach number of the maximum incremental rudder deflections and sideslip angles measured in gradual sideslips at two altitudes.

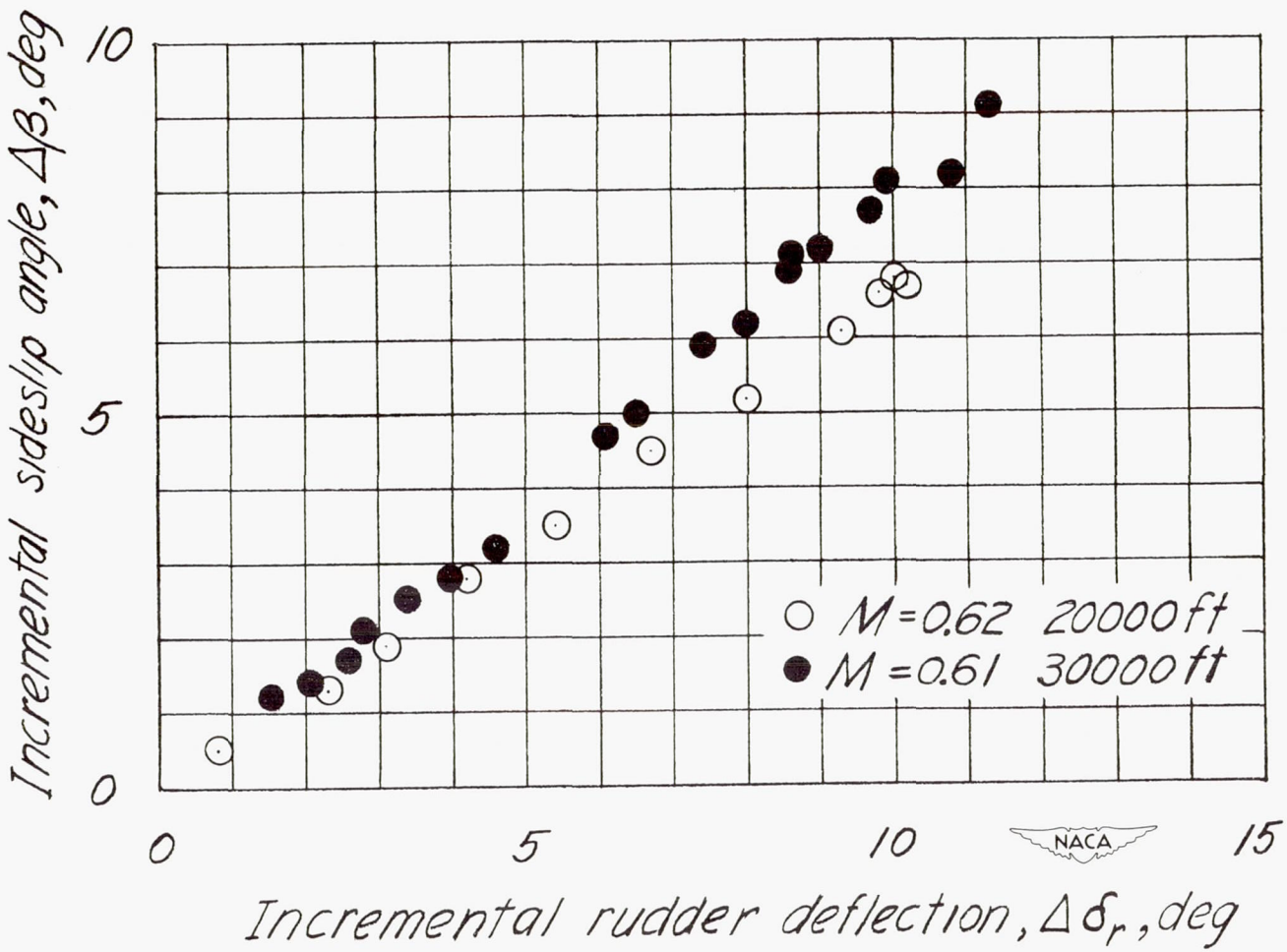

Figure 14.- Variation of incremental sideslip angle with incremental rudder angle in gradual sideslips at two altitudes.

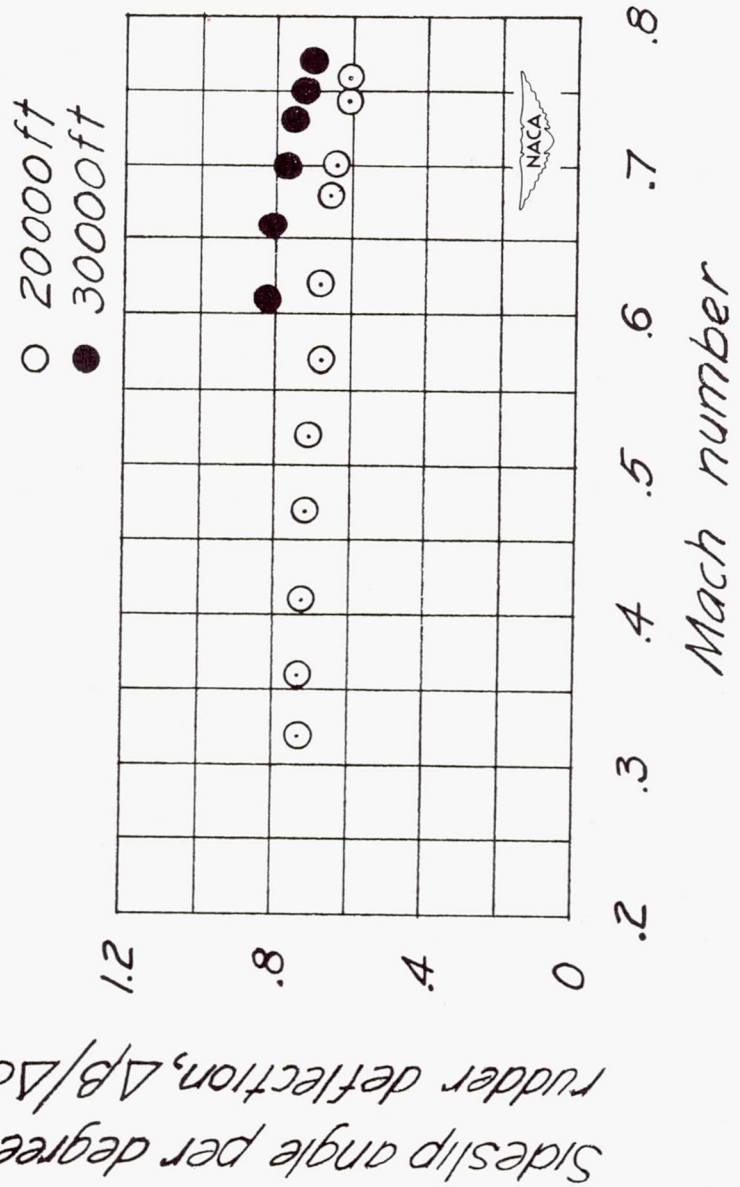

Figure 15.- Variation with Mach number of the sideslip angle per degree rudder deflection measured in gradual sideslips at two altitudes.

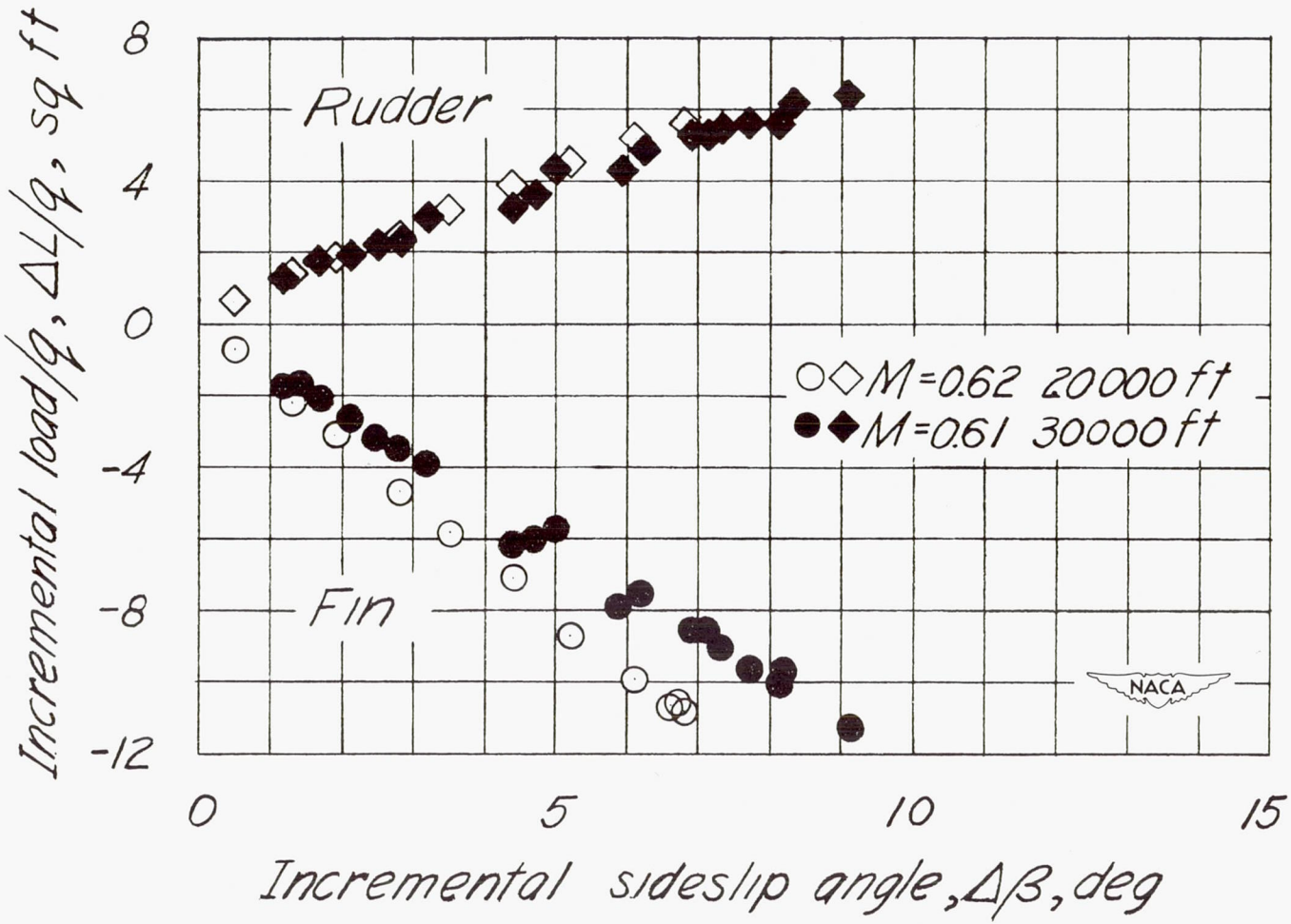

Figure 16.- Variation with incremental sideslip angle of the incremental fin and rudder loads for unit dynamic pressure measured in gradual sideslips at two altitudes.

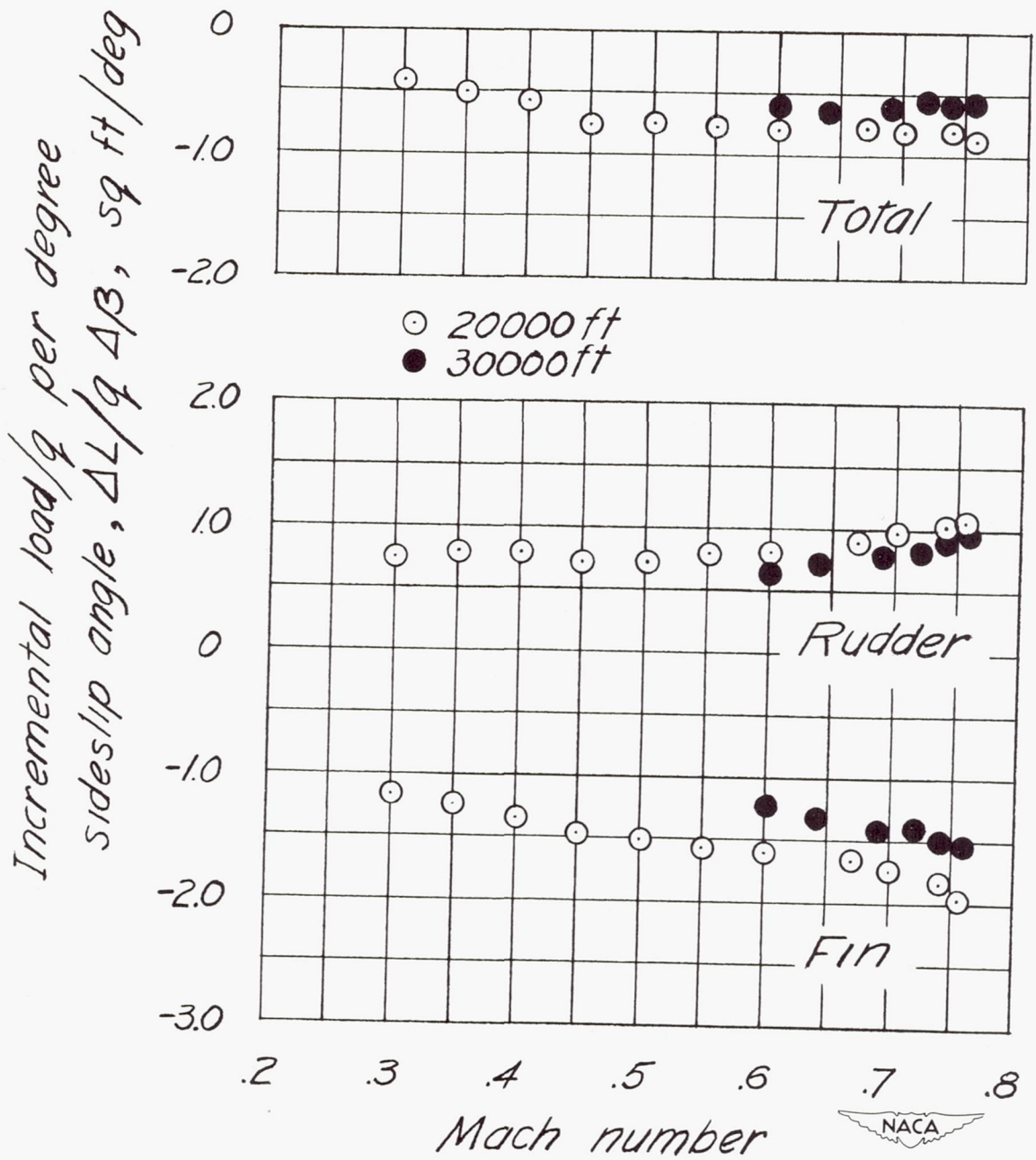

Figure 17.- Variation with Mach number of the increment in total, fin, and rudder loads for unit dynamic pressure and unit sideslip angle measured in gradual sideslips at two altitudes.

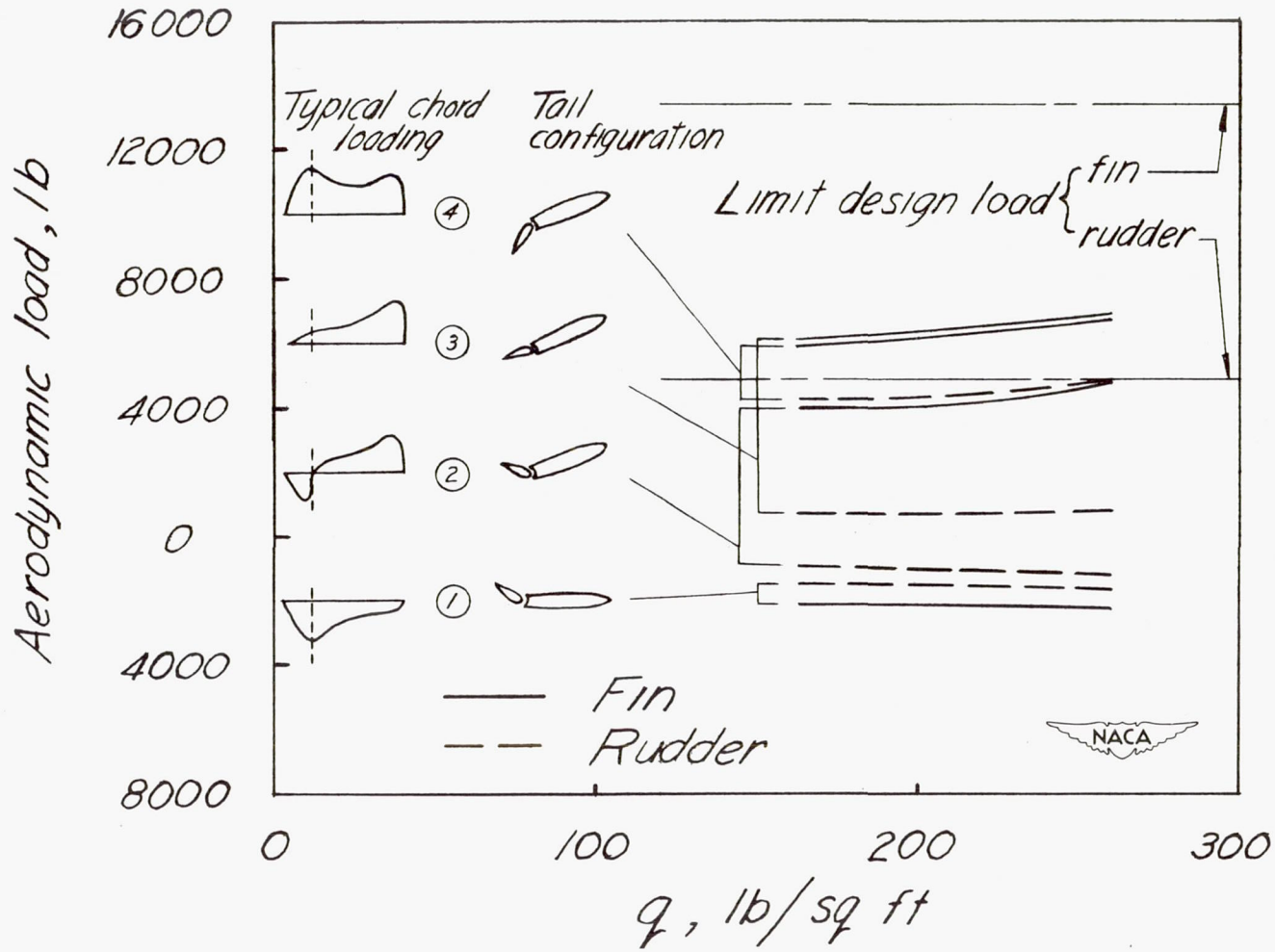

Figure 18. Calculated fin and rudder aerodynamic loads which would result at four stages of a maneuver performed by abruptly deflecting the rudder to the limiting position, holding until maximum sideslip is reached, then reversing rudder. Altitude 30,000 feet.